

## Investigation of the Stark effect in krypton autoionizing Rydberg series with the use of two-step laser excitation

Christian Delsart and Jean-Claude Keller

Laboratoire Aimé Cotton,\* CNRS II, Bâtiment 505, 91405 Orsay Cedex, France

(Received 12 July 1982)

The first detailed observation of the perturbations by an electric field of the Rydberg autoionizing resonances of a rare-gas atom is reported. The Stark spectroscopy of autoionizing Rydberg states converging to the second ionization limit  $4p^5 2P_{1/2}^0$  in Kr I is performed in an atomic beam with the use of a two-step laser excitation from the  $4p^5 5s [3/2]_2^0$  metastable state. In addition to the verification of the  $(n^*)^{-3}$  dependence of the zero-field width of two autoionizing series and of the linear dependence of the Stark-manifold splittings with the electric field, we have observed an  $(n)^{0.7}$  law for the dependence of the Stark-manifold splitting along the series, an important narrowing and dissymmetrization of the  $nd'$  resonances, and a nonlinear-field behavior of Stark-manifold components in the vicinity of the first anticrossing. Discussions are carried out with the use of the recent work on Rydberg-Stark spectroscopy and on autoionizing states in two-electron atoms.

### INTRODUCTION

Much work has been done recently on atomic Rydberg states owing to the development of multichannel quantum-defect theory (MQDT) and experimental multi-quantum laser spectroscopy.<sup>1</sup> In particular, the effects of an electric field on the Rydberg states have been extensively investigated for the alkali-metal atoms under the two main aspects, Stark structure spectroscopy and continuum Stark spectroscopy (see, for example, Refs. 2–6). In atomic systems with more than one optically active electron, the autoionizing (AI) resonances above the first ionization limit have been studied for years.<sup>7</sup> Recently some effects of static electric fields on doubly excited autoionizing Rydberg states of alkaline-earth atoms have been reported.<sup>8,9</sup> But the Stark effect of AI Rydberg series in the rare gases between the two ionization limits  $4p^5 2P_{3/2}^0$  and  $4p^5 2P_{1/2}^0$  remains unexplored except for the first observations of Cole *et al.*<sup>10</sup> on xenon at very low resolution ( $\simeq 60 \text{ cm}^{-1}$ ).

Among the rare gases, the krypton atom has been the subject of extensive experimental and theoretical investigation on its Rydberg series.<sup>11</sup> Autoionizing Rydberg series converging to the second ionization limit  $2P_{1/2}^0$  have been observed from the ground state by absorption ( $4p^5 nd' [3/2]_1^0$  and  $4p^5 ns' [1/2]_1^0$  series),<sup>12</sup> and by laser near-uv excitation from the metastable states ( $4p^5 np'$  and  $4p^5 nf'$  series).<sup>13</sup> The Beutler-Fano AI resonances have been theoretically studied using the relativistic multichannel quantum-defect theory.<sup>14</sup>

We have chosen to study the Stark effect of AI Rydberg states by a two-step laser excitation from

the metastable level  $4p^5 2P_{3/2}^0 5s [3/2]_2^0$  via the intermediate level  $4p^5 2P_{1/2}^0 5p' [1/2]_1$ . Indeed, a preliminary experiment done with the intermediate level  $4p^5 2P_{3/2}^0 6p [1/2]_1$  has shown us that the  $2P_{1/2}^0$  core AI spectrum cannot be observed due to the high purity of this level.

The first step laser is tuned at the convenient transition frequency (wavelength  $\lambda_1 = 5570.3 \text{ \AA}$ ). The wavelength of the second step is continuously scanned in the (4900–5400  $\text{\AA}$ ) range, so as to probe the photoionization spectrum between the region corresponding to an effective quantum number  $n^* = 8$  ( $n^* = n - \delta = 1/\sqrt{-2E}$  where  $\delta$  is the quantum defect),  $E$  the binding energy in atomic units relative to the second ionization energy 118 284.6  $\text{cm}^{-1}$  (Ref. 12) and the region beyond the second ionization limit.

We report in this paper a detailed study of the behavior of the AI Rydberg series in an external electric field  $F$  in the range 0–3 kV/cm. The  $n^*$  and  $F$  dependence of the AI resonance energies and widths are especially measured and discussed.

### EXPERIMENT

The general scheme of our experimental arrangement is nearly the same as the one previously used in the study of krypton Rydberg series.<sup>15</sup> An atomic beam of krypton containing a part of the atoms in the metastable levels ( $\text{Kr}^*$ ) is produced by means of an electrical radio-frequency discharge burnt inside and just outside the “oven.”<sup>15</sup> The ( $\text{Kr} + \text{Kr}^*$ ) atomic beam is irradiated between a pair of electric field plates by two dye laser beams propagating in

opposite directions at right angles to the atomic beam. Both lasers are pumped by the same pulsed nitrogen laser. The first step laser, with an intracavity Fabry Perot selector is tuned to the line  $\lambda_1 = 5570.3 \text{ \AA}$  (C540A dye) and the second step laser is swept by a step-by-step rotation of the grating between  $18\,500$  and  $20\,400 \text{ cm}^{-1}$  (C500 dye). The resulting  $\text{Kr}^+$  ions produced in the AI process are accelerated towards an electron multiplier either by means of the electric field  $F$  applied between the plates, or by means of a pulsed electric field applied just after the laser pulses. The corresponding signal is then amplified by a wide-band amplifier and it is processed by a gated integrator.

The second step laser linewidth is typically  $0.5 \text{ cm}^{-1}$ , therefore adequate for the linewidth measurements presented further. An absolute wave-number calibration is obtained by recording the coincidences between the tunable laser line and reference neon lines, respectively, in the sixth and fifth orders of a grating spectrometer. The resulting spectral precision is estimated to be  $0.5 \text{ cm}^{-1}$  which is sufficient for our purpose.

## RESULTS

At zero electric field, only the  ${}^2P_{1/2}^o$  core levels  $ns'[1/2]_{0,1}^o$  and  $nd'[3/2]_{1,2}^o$  can be reached from the intermediate level  $4p^5 5p'[1/2]_1$ . A dc electric field produces a mixing of wave functions with different  $l$ , thus allowing transition to the levels  $np'[1/2]_1$ ,  $np'[3/2]_{1,2}$ , and  $nf'[5/2]_2$  in the field range where  $J$  remains a good quantum number. As the Stark shift of the intermediate  $2p_3$  level is negligible for the field strengths used in this study, the spectrum gives directly the Stark behavior of the AI resonances. In "weak" fields, the three  $l$  states with non-negligible quantum defect  $\delta$  ( $ns'$ ,  $np'$ , and  $nd'$ ) exhibit quadratic Stark effect, whereas states with negligible  $\delta$  ( $l \geq 3$ ) form hydrogenlike manifolds with a linear Stark effect and a total number of

$n-3$  components excluding the  $l=0,1,2$  values.

A typical example of the effect of an electric field on low configurations in the vicinity of the manifold  $n=9$  is shown in Fig. 1. Contrary to the photoionization spectrum from the ground state the AI resonances are symmetrical and do not exhibit any Beutler-Fano profile for  $F=0-3 \text{ kV/cm}$ . This specific feature is connected with the absence of any photoionization continuum outside the AI resonances. Such behavior of the photoionization spectrum indicates that there is no admixture of  ${}^2P_{3/2}^o$  core contributions in the wave function of the intermediate state  $4p^5 5p'[1/2]_1$ .

As expected, the manifold  $n=9$  exhibits six equidistant components. The assignment of the observed AI resonances can be deduced from the zero-field spectrum, taking into account the previous results on the photoionization spectrum from the ground state of Kr I. According to Ref. 12, the level  $12s'[1/2]_1^o$  corresponds to a measured effective quantum number  $n^* = 8.906$  ( $\delta = 3.094$ ). The side line of the  $12s'$  resonance is assigned to the level  $12s'[1/2]_0^o$  for  $n^* = 8.896$  ( $\delta = 3.104$ ). The line which appears in the low-wavelength side of the  $10d'$  AI resonance is assigned to the  $10d'[3/2]_1^o$  level corresponding to  $n^* \simeq 8.78$  ( $\delta = 1.22$ ) according to Ref. 12. The  $10d'$  line peak ( $n^* = 8.64$ ,  $\delta = 1.36$ ) can be identified to the  $10d'[3/2]_2^o$  and  $10d'[5/2]_2^o$  levels (expected energy distance  $1-2 \text{ cm}^{-1}$ ).

In the presence of an electric field (Fig. 1), the  $11p'$  AI resonance which appears by  $l$  mixing ( $n^* = 8.38$ ,  $\delta = 2.62$ ) could be assigned to the levels  $11p'[3/2]_{1,2}$  according to the extrapolated values of Ref. 13 and assuming that  $J$  remains a good quantum number. In the same conditions, the Stark manifold would correspond to the  $9f'[5/2]_2$  level. In the vicinity of the second ionization limit  ${}^2P_{1/2}^o$ , the zero-field photoionization spectrum shown in Fig. 2 exhibits the classical convergence of the series to the limit, and, moreover, a regular decreasing of the AI resonance widths. Figure 3 reports the mea-

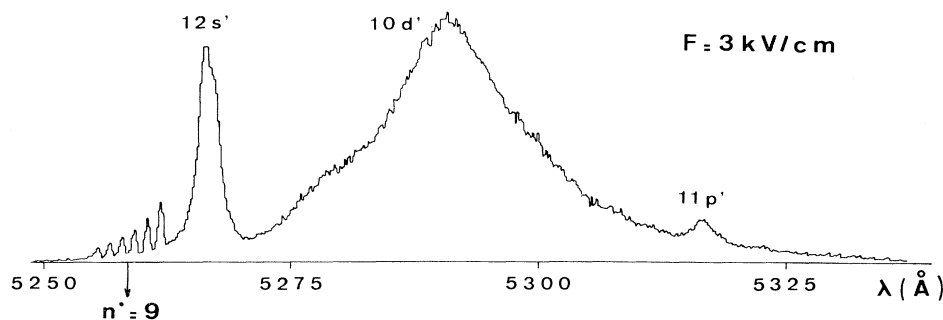


FIG. 1. Photoionization spectrum from level  $4p^5 5p'[1/2]_1$  in an electric field  $F = 3 \text{ kV/cm}$  in the range  $8 < n^* \leq 9$  ( $n^* = 1/\sqrt{-2E}$  is the effective quantum number,  $E$  is the binding energy relative to the second ionization limit in atomic units).

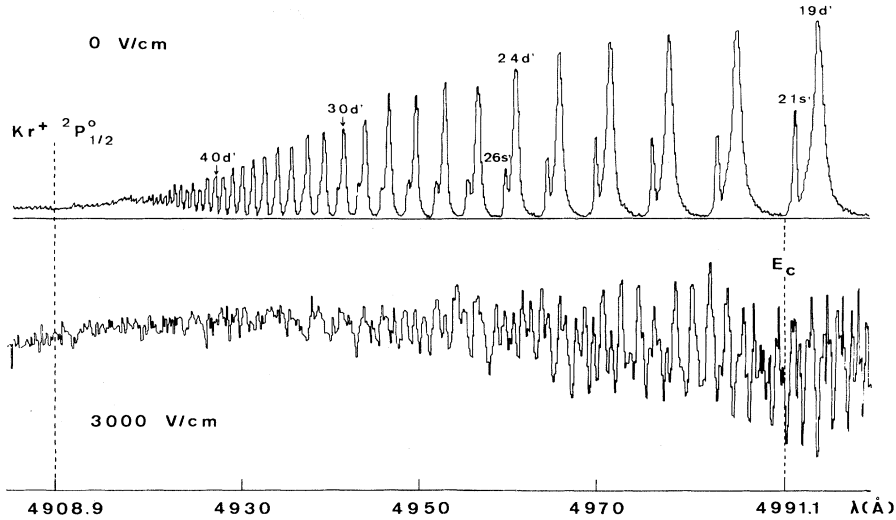


FIG. 2. Comparison of the photoionization spectra from level  $4p^5 5p'[1/2]_1$  at zero field and at  $F=3$  kV/cm in the vicinity of the second ionization limit.  $E_c = -2\sqrt{F}$  (a.u.) is the critical binding energy relative to the second ionization limit.

sured zero-field  $ns'$  and  $nd'$  resonance widths  $\Delta\sigma$  as a function of the effective quantum number  $n^*$ . The expected  $(n^*)^{-3}$  dependence<sup>1,16</sup> of the AI linewidth is remarkably well verified, especially for  $nd'$  between  $9d'$  ( $\Delta\sigma=68$  cm<sup>-1</sup>) and  $26d'$  ( $\Delta\sigma=2.4$  cm<sup>-1</sup>). We obtain the following values for the  $nd'$  and  $ns'$  linewidths:

$$\Delta\sigma_{nd'} = 3.3 \times 10^4 (n^*)^{-3} \text{ cm}^{-1},$$

$$\Delta\sigma_{ns'} = 0.62 \times 10^4 (n^*)^{-3} \text{ cm}^{-1}.$$

These results can be connected to the width parameter  $\Gamma$  deduced from the parametric Fano formula in the studies of the photoionization cross sections

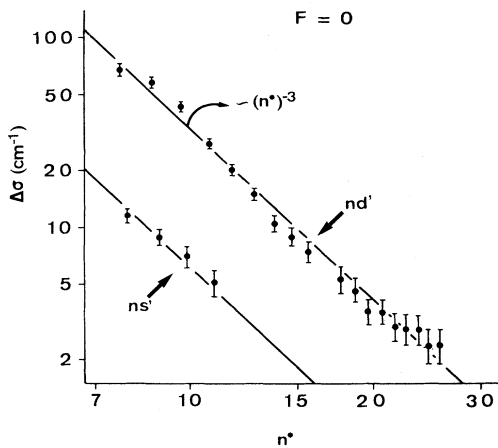


FIG. 3. Measured zero-field  $ns'$  and  $nd'$  AI resonance widths  $\Delta\sigma$  plotted vs  $n^*$  on logarithmic scales.  $(n^*)^{-3}$  dependence is indicated by the dark lines. Mean values of the quantum defects  $\delta = n - n^*$  are  $\delta_{d'}=1.3$  and  $\delta_{s'}=3.1$  for the  $nd'$  and  $ns'$  resonances.

from the ground state in krypton.<sup>14,17</sup> However, due to the low instrumental resolution, only  $\Gamma_{nd'}$  has been measured in a limited region and it has been shown that the product  $\Gamma_{nd'}(n^*)^3$  varies smoothly from  $2.12 \times 10^4$  cm<sup>-1</sup> for  $n=6$  to  $1.92 \times 10^4$  cm<sup>-1</sup> for  $n=14$ .<sup>17</sup>

The photoionization spectrum in the presence of an electric field  $F$  on Fig. 2 shows that the “critical” energy  $E_c = -2\sqrt{F}$  (in atomic units) relative to the second ionization limit, defined in the classical saddle-point model<sup>1</sup> plays no significant part. This indicates the predominance of the autoionization process on the field-induced photoionization process. Another point is the fast vanishing of the Stark modulations<sup>3,5,18</sup> below the second ionization limit. It has been found that both zero-field and field photoionization spectra do not change appreciably with the laser polarization, which proves that a large mixing of the  $m_l$  values in the starting and final states exists. This unfavorable feature explains the decrease of the contrast due to the superposition of different  $m$  contributions and also fixes the limits of the present experiment.

Accounting for these considerations, we have performed an extensive experimental study of the Stark structure in the region  $n=13-15$  where the level crossings appear just for  $F=3$  kV/cm. Figure 4 shows some recordings illustrating the field behavior of the AI resonances. It can be seen that the Stark-manifold components exhibit field-independent linewidths (mean value  $2$  cm<sup>-1</sup>), an observation which agrees with the results in barium.<sup>8</sup> In this field and energy range, the  $ns'$  and  $np'$  resonances are little altered when the  $nd'$  resonances are drastically narrowed and “absorbed” in the neighboring

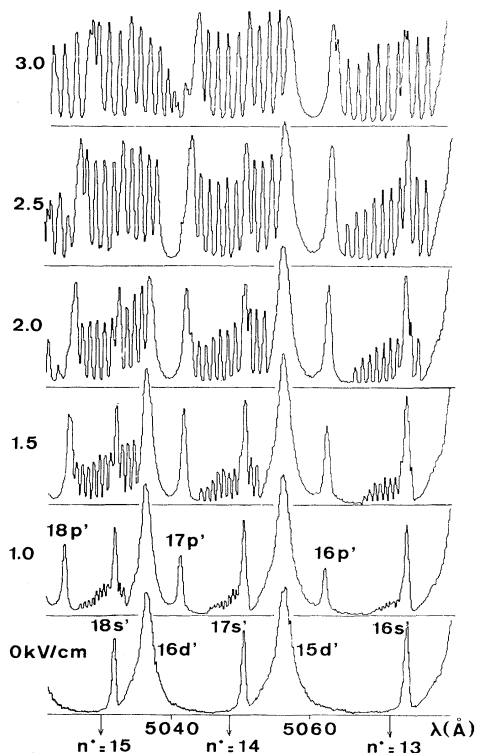


FIG. 4. Evolution of the photoionization spectrum from level  $4p^5 5p'[1/2]_1$  for  $F=0, 1, 1.5, 2, 2.5, 3$  kV/cm in the  $n^*=13-15$  region.

Stark manifold. Figure 5 illustrates the fast decrease of the 15–17  $d'$  linewidths to a bound value of about  $2 \text{ cm}^{-1}$  which is precisely the mean linewidth of the manifold components. This phenomenon is related to the first anticrossing with the near Stark manifold. Indeed it is well known<sup>4</sup>

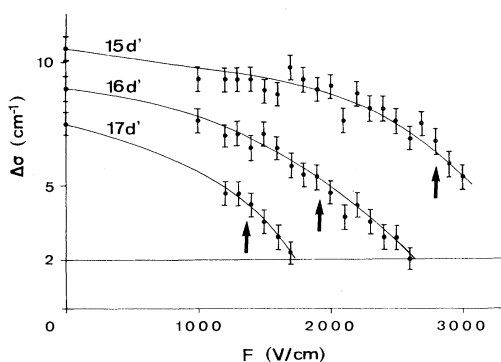


FIG. 5. Electric field behavior of the  $nd'$  AI resonance widths near the anticrossing with the  $(n-1)$  manifold. Arrows give the expected approximate value  $F=1/5(n-2)^5$  for the first anticrossing. The horizontal line gives the common mean value ( $2 \text{ cm}^{-1}$ ) of the  $\Delta\sigma$  minimum value and of the manifold component linewidth.

that the first anticrossing between the manifolds  $n$  and  $n+1$  occurs at a field value  $F \approx 1/3n^5$ . In our case, the first anticrossing between the  $nd'$  level which has a quantum defect  $\delta_{d'} \approx 1.36$  and the lower component of the  $(n-1)$  Stark manifold can be expected roughly at a field value  $F \approx 1/5(n-2)^5$ . Figure 5 shows that for these indicative values the measured linewidths are about 60% that of the zero-field AI resonance widths for  $n=15-17$ . Moreover, the narrowing effect coincides with an important dissymmetrization of the resonance shape (Fig. 4). These two effects can be analyzed as phenomena involving totally mixed wave functions in the region of the avoided crossing.<sup>9</sup> As the manifold lines are much narrower than the  $nd'$  resonances, the field-induced admixture of the various angular momentum states leads to a narrowing of the  $nd'$  resonances with some interference effects in the anticrossing region explaining the dissymmetry.

The Stark map, i.e., the experimental Stark energy diagram is reported in Fig. 6 for the same spectral range, so as to point out the main properties of the manifolds. Except in the vicinity of the anticrossings, the  $n$  manifold exhibits the classical linear field dependence (at least from  $F=1$  kV/cm), the same for all  $m$  values as for the alkali metals.<sup>4</sup>

We have also performed a test of the validity in the case of krypton of the classical hydrogenic linear  $n$  dependence of the splitting  $\delta\sigma$  between two adja-

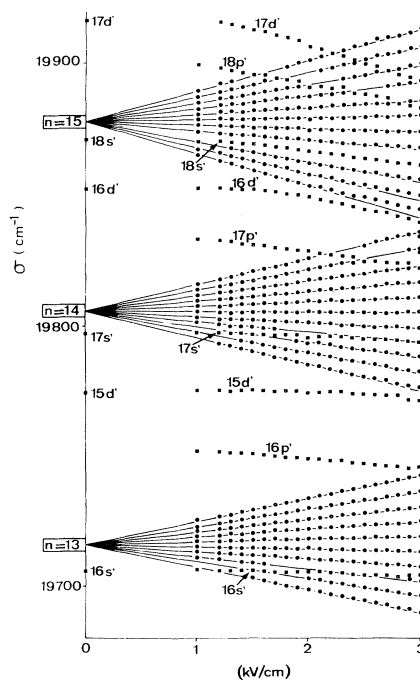


FIG. 6. Experimental Stark structure of the AI resonances in the  $n^*=13-15$  region. ●: Manifold components; ■:  $ns'$ , and  $np'$ , and  $nd'$  resonances.

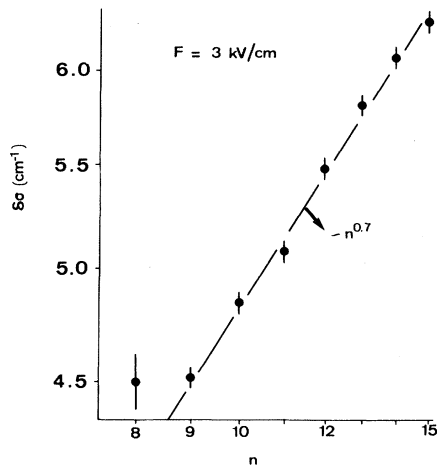


FIG. 7. Measured splitting  $\delta\sigma$  between the Stark-manifold components at  $F=3$  kV/cm plotted vs  $n$  on logarithmic scales. Dark line corresponds to an  $n^{0.7}$  law. Measurement of the  $n=8$  value suffers from the weak intensity of the manifold at  $F=3$  kV/cm.

cent levels of the same  $n$  manifold. The measured splitting  $\delta\sigma$  at  $F=3$  kV/cm for  $n=8-15$  is plotted versus  $n$  in Fig. 7 with logarithmic scales. The slope  $0.70 \pm 0.05$  has been confirmed for other values of the electric field. The interpretation of this surprising nonhydrogenic  $n^{0.7}$  behavior, which entails important computational techniques, is beyond the scope of this paper.

Figures 4 and 6 also show the appearance at 3 kV/cm of two additional lines near the upper components of the Stark manifold  $n=14$ . Indeed, it has been shown recently<sup>4</sup> that level separations at an-

ticrossings are sensitive functions of the quantum defects, vanishing as the decimal part of the quantum defects approach 0 or 1. Here the main contributions to the anticrossings are produced by the  $np'$  ( $\delta_{p'} \approx 2.62$ ) and  $nd'$  ( $\delta_{d'} \approx 1.36$ ), and then the level repulsions must be markedly stronger for the cases  $|m_l|=0,1$  than for  $|m_l|=2$  and, moreover, for  $|m_l| \geq 3$ . It can be reasonably assumed that the lines following the linear field dependence correspond to  $|m_l| \geq 2$  and the repulsed neighboring lines correspond to  $|m_l| < 2$ . Such a shift arises also for the lower components of the Stark manifolds  $n=14$  and  $n=15$  at the anticrossings with  $15d'$  and  $16d'$  levels.

In summary, we have demonstrated experimentally the effect of electric fields on the autoionizing Rydberg resonances of the  $^2P_{1/2}^o$  excited core in Kr I. As in the alkaline-earth metals, the shapes, widths, and shifts of AI resonances are strongly perturbed by the Stark effect.

However, the effects of the electric field can be understood in terms of the interpretation of the Stark effect for bound Rydberg levels. This observation implies that the electric field affects the Rydberg electron, but not the excited  $^2P_{1/2}^o$  core. The other effects on linewidths and line shapes arise from the electric field mixing of the discrete portions of the AI states with little effect on the coupling to the continuum states, in both initial and final states of the autoionizing excitation. Theoretical interpretation, in spite of its complexity and the computational difficulties, would certainly bring some further informations on the field behavior of the Kr I AI resonances.

\*This laboratory is associated with the University of Paris-Sud.

<sup>1</sup>See, for a review, S. Feneuille and P. Jacquinot, *Adv. Atom. Mol. Phys.* **17**, 99 (1981).

<sup>2</sup>R. R. Freeman, N. P. Economou, G. C. Bjorklund, and K. T. Lu, *Phys. Rev. Lett.* **41**, 1463 (1978).

<sup>3</sup>R. R. Freeman and N. P. Economou, *Phys. Rev. A* **20**, 2356 (1979).

<sup>4</sup>M. L. Zimmerman, M. G. Littman, M. M. Kash, and D. Kleppner, *Phys. Rev. A* **20**, 2251 (1979).

<sup>5</sup>T. S. Luk, L. Dimauro, T. Bergeman, and H. Metcalf, *Phys. Rev. Lett.* **47**, 83 (1981).

<sup>6</sup>S. Feneuille, S. Liberman, E. Luc-Koenig, J. Pinard, and A. Taleb, *Phys. Rev. A* **25**, 2853 (1982).

<sup>7</sup>See, for example, U. Fano and J. W. Cooper, *Rev. Mod. Phys.* **40**, 441 (1968); U. Fano, *J. Opt. Soc. Am.* **65**, 979 (1975).

<sup>8</sup>K. A. Safinya, J. F. Delpech, and T. F. Gallagher, *Phys. Rev. A* **22**, 1062 (1980).

<sup>9</sup>R. R. Freeman and G. C. Bjorklund, *Phys. Rev. Lett.*

**40**, 118 (1978).

<sup>10</sup>B. E. Cole, J. W. Cooper, D. L. Ederer, G. Mehlman, and E. B. Saloman, *J. Phys. B* **13**, L175 (1980).

<sup>11</sup>M. Aymar, O. Robaux, and C. Thomas, *J. Phys. B* **14**, 4255 (1981), and bibliography therein.

<sup>12</sup>K. Yoshino and Y. Tanaka, *J. Opt. Soc. Am.* **69**, 159 (1979).

<sup>13</sup>F. B. Dunning and R. F. Stebbings, *Phys. Rev. A* **9**, 2378 (1974).

<sup>14</sup>W. R. Johnson, K. T. Cheng, K. N. Huang, and M. Le Dourneuf, *Phys. Rev. A* **22**, 987 (1980).

<sup>15</sup>C. Delsart, J. C. Keller, and C. Thomas, *J. Phys. B* **14**, 4241 (1981).

<sup>16</sup>See, for example, W. R. S. Garton, G. L. Grasdalen, W. H. Parkinson, and E. M. Reeves, *J. Phys. B* **1**, 114 (1968).

<sup>17</sup>K. Radler and J. Berkowitz, *J. Chem. Phys.* **70**, 216 (1979).

<sup>18</sup>D. A. Harmin, *Phys. Rev. A* **24**, 2491 (1981).